Supporting Information

Defect engineering in atomically-thin bismuth oxychloride towards photocatalytic oxygen evolution

Jun Di[1,2], Chao Chen[2], Shi-Ze Yang[3], Mengxia Ji[1], Cheng Yan[2], Kaizhi Gu[4], Jiexiang Xia[1,*], Huaming Li[1], Shuzhou Li[2], Zheng Liu[2,*]

[1] School of Chemistry and Chemical Engineering, Institute for Energy Research, Jiangsu University, 301 Xuefu Road, Zhenjiang, 212013, P. R. China

[2] Center for Programmable Materials, School of Materials Science & Engineering, Nanyang Technological University, Singapore 639798, Singapore

[3] Materials Science and Technology Division, Oak Ridge National Laboratory, USA

[4] School of Chemistry and Molecular Engineering, East China University of Science and Technology, Shanghai 200237, P. R. China

*Corresponding author: z.liu@ntu.edu.sg; xjx@ujs.edu.cn

The details of density functional theory (DFT) calculations

Code: GPAW

Method: projector-augmented wave (PAW)

Basis: Plane wave

Pseudopotential: PBE

Convergence criterion:

Energy: 0.0005, # eV / electron

Density: 1.0e-4,

Eigenstates: 4.0e-8, # eV^2 / electron

Bands: occupied,

Forces: float('inf')} # eV / Ang Max

k-points:

bulk material: 12*12 *12 f

(001) 2d surface 12 *12 *1

(110) 1d surface 1*12 *1

Defect rich surface 1*12 *1

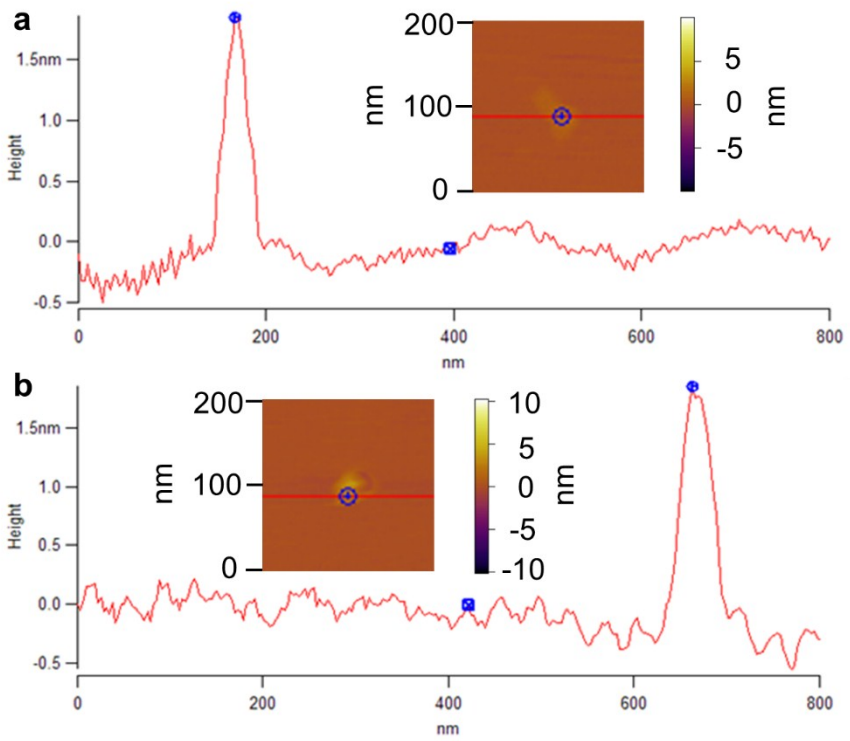

Figure S1. AFM images of (a) BiOCl materials and (b) defect-rich BiOCl ultrathin nanosheets.

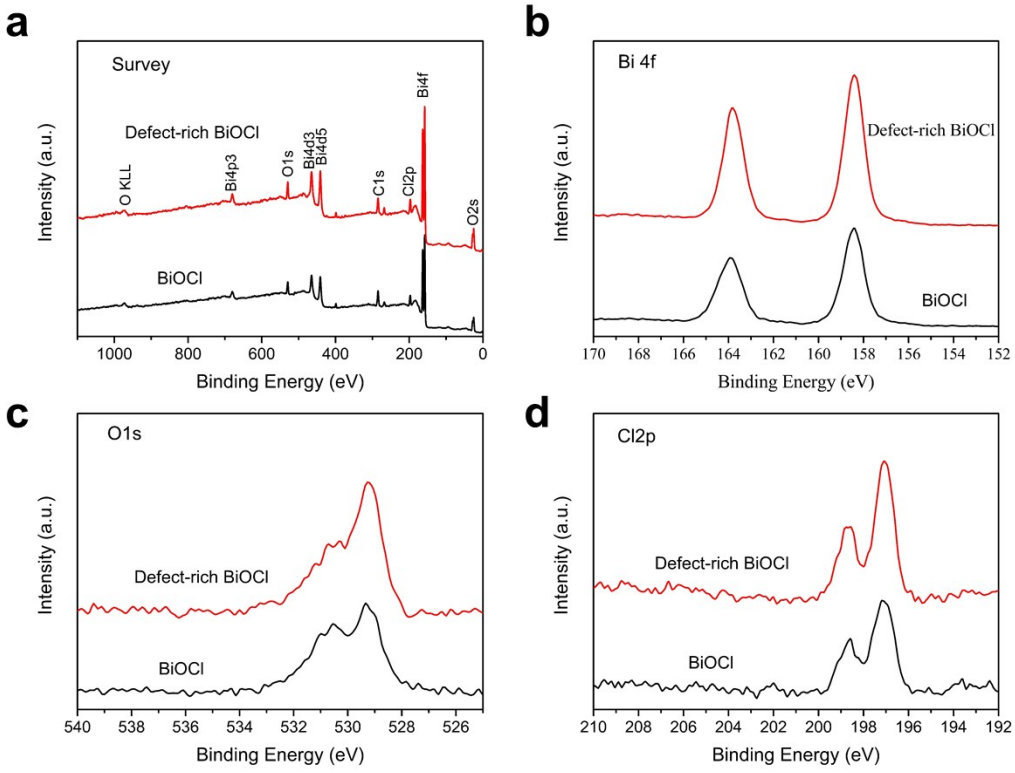

Figure S2. XPS spectra of BiOCl and defect-rich BiOCl materials, (a) Survey of the sample, (b) Bi 4f, (c) O 1s, (d) Cl 2p.

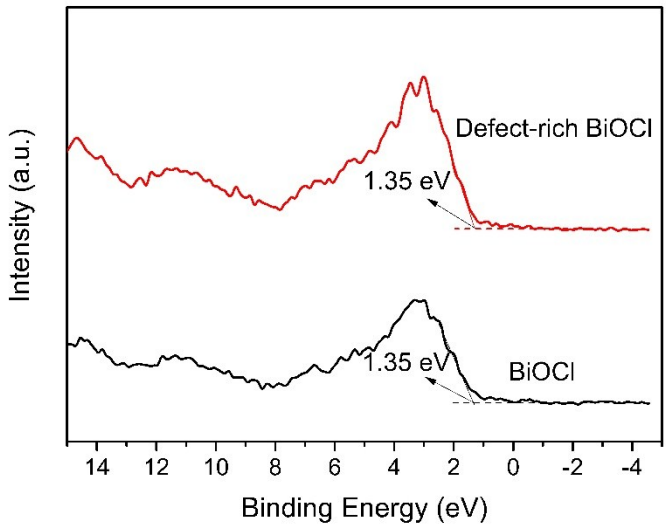

Figure S3. XPS valence band spectra of BiOCl and defect-rich BiOCl.

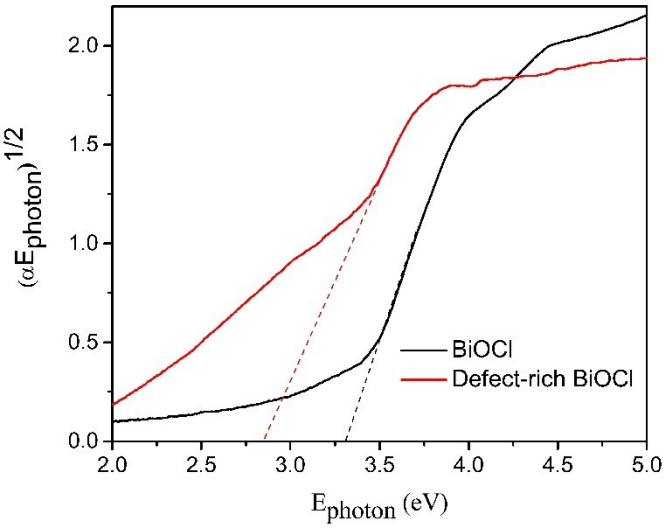

Figure S4. $(\alpha E_{photon})^{1/2}$ vs. E_{photon} curves of the as-prepared BiOCl and defect-rich BiOCl sample.

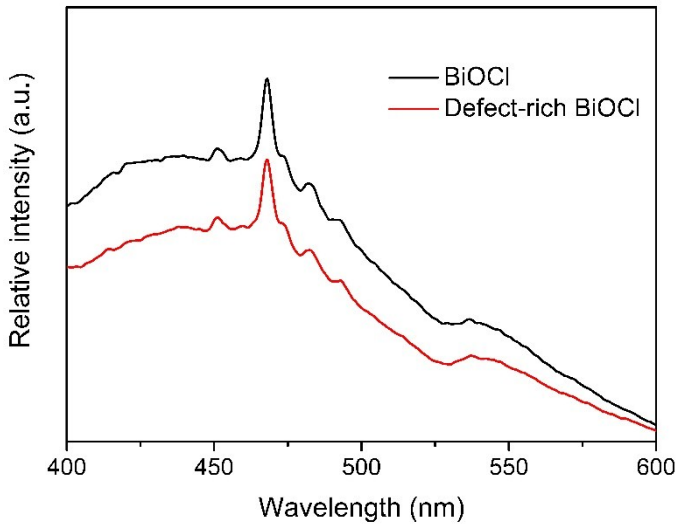

Figure S5. Steady-state photoluminescence (PL) spectra of the BiOCl and defect-rich BiOCl materials.

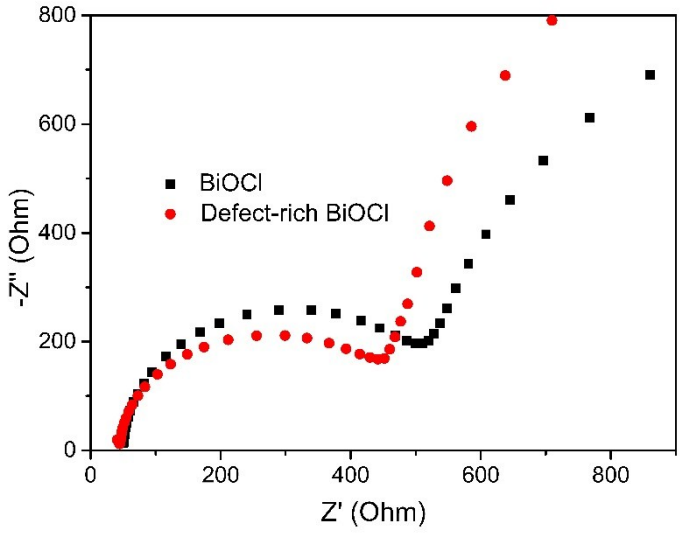

Figure S6. Electrochemical impedance spectroscopy (EIS) of BiOCl and defect-rich BiOCl materials.

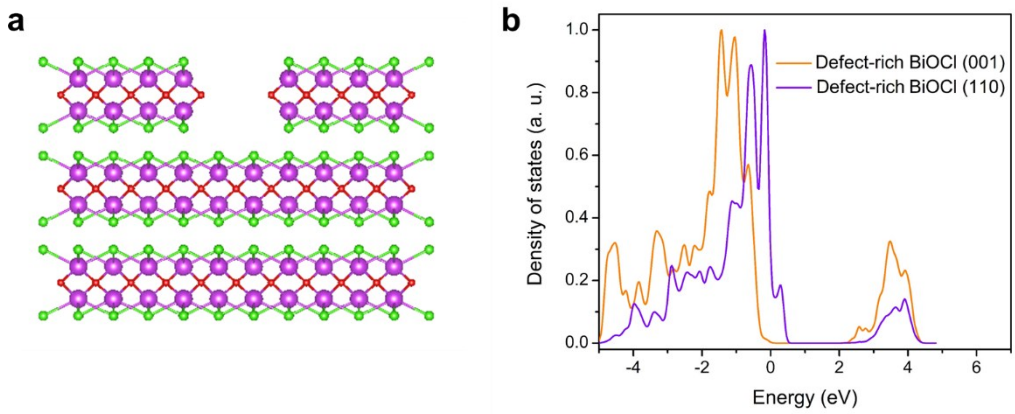

Figure S7. (a) Crystal structure of defects-rich BiOCl, (b) DOS diagrams from first-principles simulations for defects-rich BiOCl (001) and defects-rich (110) facets.

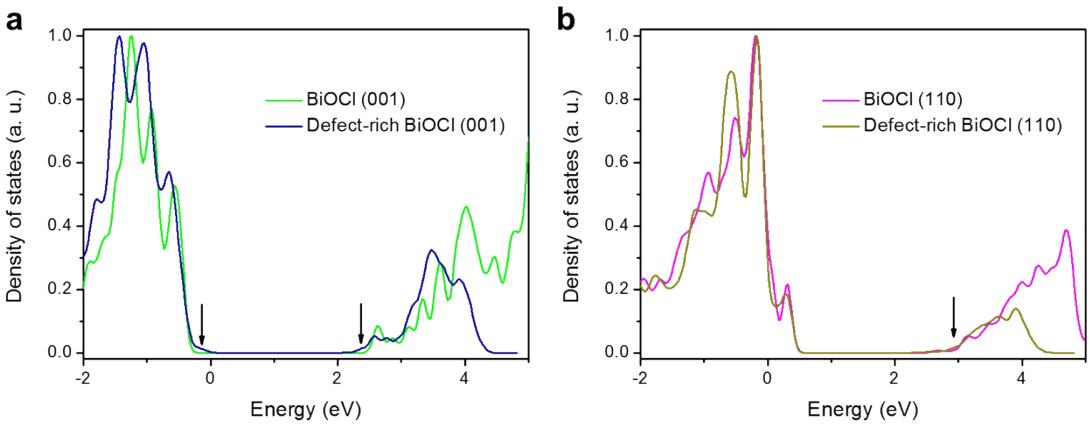

Figure S8. Calculated DOS of atomically-thin BiOCl nanosheets and defect-rich BiOCl, (a) (001) and (b) (110) facets.

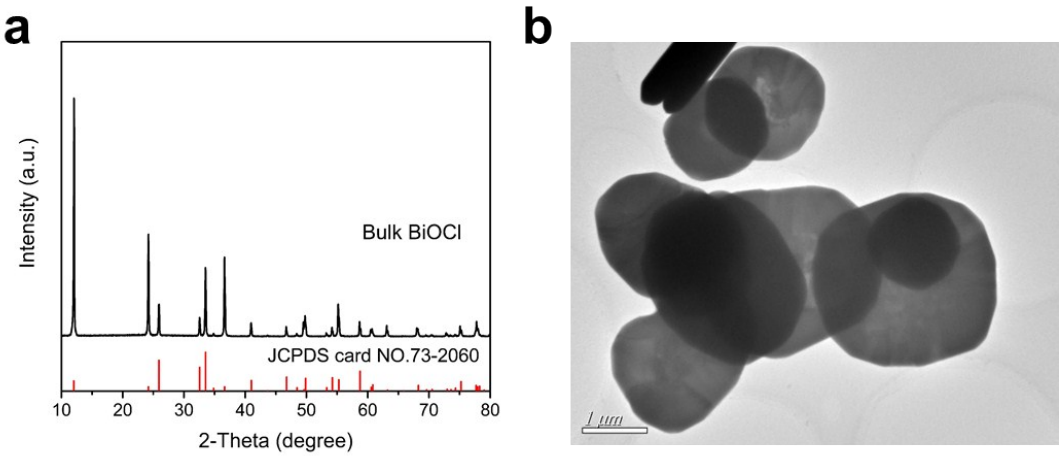

Figure S9. Characterizations of bulk BiOCl. (a) XRD pattern and (b) TEM image.

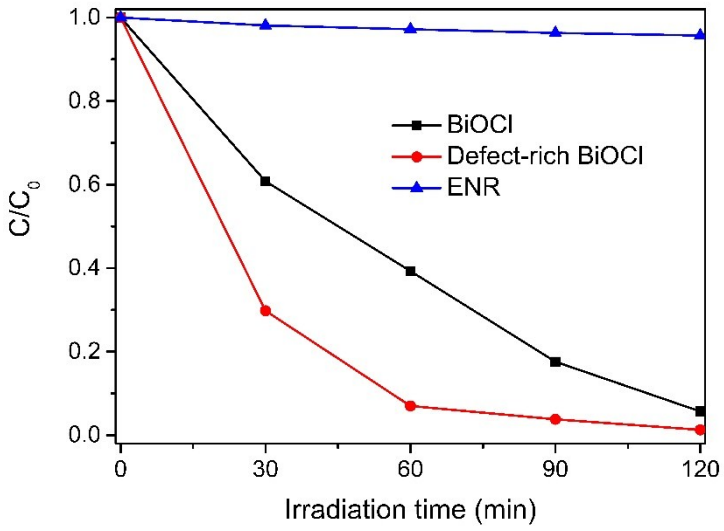

Figure S10. Photocatalytic degradation of ENR in the presence of BiOCl and defect-rich BiOCl materials under light irradiation.

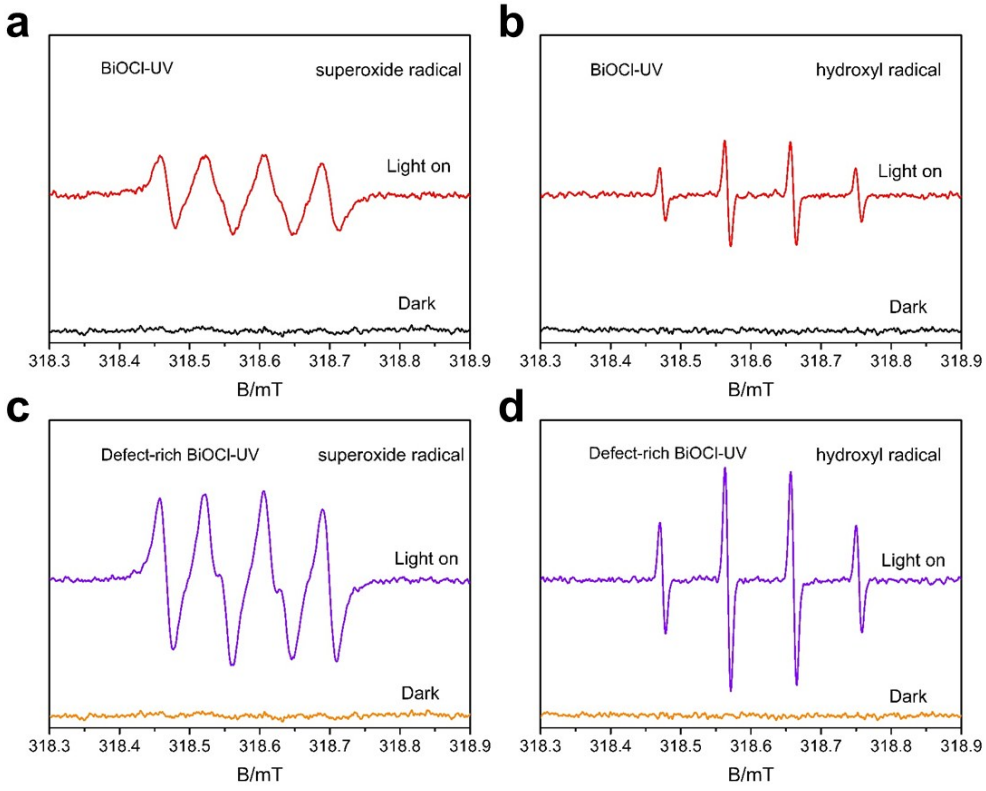

Figure S11. ESR spectra of the DMPO-$O_2^{\bullet-}$ adducts and DMPO-·OH recorded with (a, b) BiOCl and (c, d) defect-rich BiOCl under UV light irradiation.